Journal of Computational Applied Mechanics 2021, 52(1)
DOI: 10.22059/jcamech.2019.288900.429

RESEARCH PAPER

# Slip effect on the unsteady electroosmotic and pressure-driven flows of two-layer fluids in a rectangular microchannel.

**Abdul Rauf [1,*], Yasir Mahsud[2]**

[1] *Dept. of Computer Science and Engineering, Air University Multan, Pakistan*

[2] *Abdus Salam School of Mathematical Sciences, GCU Lahore, Pakistan*

## Abstract

Electroosmotic flows of two-layer immiscible Newtonian fluids under the influence of time-dependent pressure gradient in the flow direction and different zeta potentials on the walls have been investigated. The slippage on channel walls is, also, considered in the mathematical model. Solutions to fluid velocities in the transformed domain are determined by using the Laplace transform with respect to the time variable and the classical method of the ordinary differential equations. The inverse Laplace transforms are obtained numerically by using Talbot's algorithm and the improved Talbot's algorithm.

Numerical results corresponding to a time-exponential pressure gradient and translational motion with the oscillating velocity of the channel walls have been presented in graphical illustrations in order to study the fluid behavior. It has been found that the ratio of the dielectric constant of fluid layers and the interface zeta potential difference have a significant influence on the fluid velocities.

**Keywords:**

Electroosmotic flow; slip condition; layer flows; Newtonian fluids.

## 1. Introduction

The study of microfluidic devices is important due to its vital applications in analytical chemistry, biology, and medical science [1]. The microchannel wall under the influence of electrolyte produces the surface charges, which results in the formulation of an electrical double layer (EDL) and the resulting ion density variation satisfies the Boltzmann distribution [2, 3]. The application of the tangential electric field on the charged microchannel leads to a Coulombic force on the ions within an electrical double layer. Due to the viscosity, the net migration of the mobile ions will carry the adjacent and bulk liquid which results in an electroosmotic flow (EOF).

EOF received considerable attention due to its wide applications in a variety of microfluidic devices used in the medical and biochemical analysis. The ability of EOF to build pressure make it favourable to use in a pumping mechanism involve in microchannel geometries for bioanalytical [4, 5] and electronic cooling systems [6]. Dutta and Beskok [7] considered the time-periodic EOF in a 2-D channel consisting of parallel plates and found its

* Corresponding Author. Tel.: +92 (61) 4780091 Ext: 170
*Email Address*: abdul.rauf@aumc.edu.pk

analytical solution consisting of the EDL thickness, frequency of external electric current and the kinematic viscosity. They discussed various similarities and dissimilarities with the Stokes second problem. Wang et al. [8] found the semi-analytical as well as the numerical solutions for the flow behaviour of periodic EOF through a rectangular microchannel. It is found that the slip velocity of periodic EOF decreases with the increase in Reynolds number. Jian et al. [9] studied the EOF of Maxwell fluid between microchannel consisting of parallel plates and found a semi-analytical solution. The time depended periodic electroosmotic flow for generalized Maxwell fluid was considered by Liu [10] and Jian [11]. Other interesting results related to EOF corresponding to the high conductivity fluids can be found in [12, 13, 14].

In order to transport a low conductivity fluid, a 2-layer fluid flow system is introduced by Brask [15]. To form such a double layer, a significantly high electrically conducted fluid drags the other fluid by the applied shear stress at the interface for the separation of the mixture. Shankar and Sharma [16] and Verma et al. [17] studied the instabilities of microfilms and highlighted the significance of Maxwell interfacial stress. Liu [18] presented a numerical study for EOF in a cylindrical coaxial microchannel under the influence of Maxwell interfacial shear stress. Gao et al [19] also considered the Maxwell stress at the interface and studied the two-layer electroosmotic flow in a rectangular channel. Later, Su et al. [20] considered the effect of zeta potential at the interface in addition to the Maxwell stress at the interface and studied the electroosmotic flow in a microchannel consisting of parallel plates. Slip boundary condition on the velocity at the solid-fluid interface is another important factor to stimulate the EOF. Goswami and Chakraborty [21] studied the electro-osmosis hydrodynamic flow of complex domain in the presence of interfacial slip. They considered the combined effect of Navier slip at the solid-fluid interface and the electroosmotic slip and found semi-analytical results. Shit et al. [22] examined numerically the EOF in a wavy micro-channel in the presence of slip boundary conditions and found a good agreement with the previously known results under no-slip condition.

In this study, we have developed a semi-analytical model to study the two-layer fluid flow under the combined effect of electroosmosis as well as the applied pressure gradient in the presence of Robin type boundary conditions at the solid-fluid interface. We also consider the influence of zeta potential difference which plays an important role in actuating the EOF. We used the Debye-Hückel approximation to linearize the governing Poisson-Boltzmann equations for zeta potential function.

## 2. Mathematical Modelling

The electro-osmotic flow domain is $\mathfrak{D}' = \{(x', y', z') \mid x' \in (-\infty, \infty), y' \in [0, d], z' \in (-\infty, \infty)\}$, with the boundary walls of slit micro channel bounded by two negatively charged parallel plates of length $L(>> d)$ situated horizontally in planes $y' = 0$ and $y' = d > 0$ (see Fig. 1 for the geometry). The flow domain is divided in two regions at $y' = d_1$. In the region $y' \in [0, d_1], 0 < d_1$ flows a Newtonian fluid with the density $\rho_1$, viscosity $\mu_1$, velocity $v_1'(y', t')$ and the shear stress $\tau_1'(y', t')$. In the region $y' \in [d_1, d], d_1 < d$ flows a Newtonian fluid with the density $\rho_2$, viscosity $\mu_2$, velocity $v_2'(y', t')$ and the shear stress $\tau_2'(y', t')$.

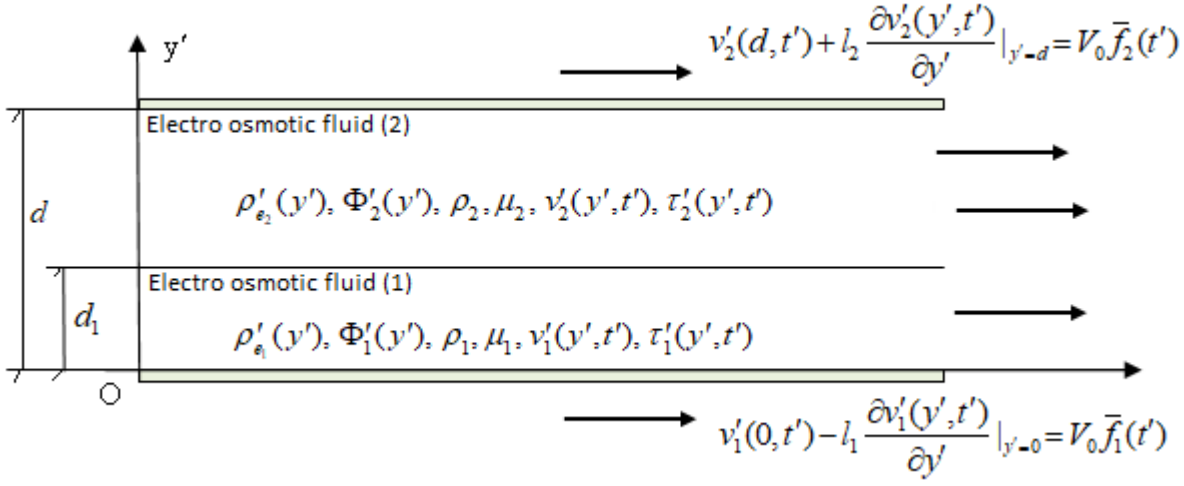


Figure 1: Geometry of the problem.

Initially, at time $t'=0$, the fluid in both regions is at rest. After time $t'=0^+$, the electro-osmotic flow is driven along $x'$-axis by applied pressure gradient $-\frac{\partial p'}{\partial x'}$ and an axial direct current (DC) electric field of strength $E$ as shown in Fig. 1. The Poisson-Boltzmann equations describe the electric potential distribution $\Phi_i'(y'), i=1,2,$ and the local volumetric net charge density $\rho_{e_i}'(y')$ produced within both regions due to the presence of electrical double layer in a micro-channel are given by

$$\frac{\rho_{e_i}'(y')}{\varepsilon_i}=-\frac{d^2\Phi_i'(y')}{dy'^2},\ i=1,2, \tag{1}$$

$$\rho_{e_i}'(y')=-2z_v n_0 e\sinh\left(\frac{z_v e}{T_o K_B}\Phi_i'\right),\ i=1,2, \tag{2}$$

where $e, z_v$ are the electric and valance charge, $n_0$ is the ion density of the bulk liquid, $T_o$ is the absolute temperature and $K_B$ is the Boltzmann constant. For a small value of the electric potential, and with the help of Eqs. (1) and (2), we get Deybe-Hückel equation by linear approximation of sine hyperbolic function

$$\frac{d^2\Phi_i'(y)}{dy'^2}=K_i^2\Phi_i'(y),\ i=1,2, \tag{3}$$

where $K_i^2=\frac{2z_v^2 n_0 e^2}{T_o K_B \varepsilon_i}$ and $\frac{1}{K_i}$ represents the thickness of electrical double layer. The boundary conditions for electrical potential distribution $\Phi_i'$ are

$$\Phi_1'(0)=\Phi_0',\ \Phi_2'(d)=\Phi_s', \tag{4}$$

where $\Phi'_0$ and $\Phi'_s$ are the wall zeta potential. The interface fluid-fluid conditions for electrical potential distribution are given by Gauss's law and zeta potential difference $\Delta\Phi'$ and are

$$\varepsilon_1 \frac{d\Phi'_1(y')}{dy'}|_{y'=d_1} - \varepsilon_2 \frac{d\Phi'_2(y')}{dy'}|_{y'=d_1} = -Q_s,\ \Phi'_2(d_1) - \Phi'_1(d_1) = \Delta\Phi', \tag{5}$$

where $Q_s$ is the interfacial charge density jump. Consider the following non-dimensional variables,

$$\begin{gathered} 6y = \frac{y'}{d}, \Phi_i = \frac{\Phi'_i}{A}, \Phi_0 = \frac{\Phi'_0}{A}, \Phi_s = \frac{\Phi'_s}{A}, \Delta\Phi = \frac{\Delta\Phi'}{A}, A = \frac{K_B T_o}{z_v e}, \\ \varepsilon = \frac{\varepsilon_2}{\varepsilon_1}, D = \frac{d_1}{d}, Q = \frac{z_v Q_s e d}{K_B \varepsilon_1 T_o}, k_i = dK_i,\ i = 1,2. \end{gathered} \tag{6}$$

where $k_i$ represents the ratio between characteristic scale of the channel width to Debye length. Eqs (3), (4) and (5) in the dimensionless form reduce to

$$\frac{d^2\Phi_i(y)}{dy^2} = k_i^2 \Phi_i(y),\ i = 1,2, \tag{7}$$

$$\Phi_1(0) = \Phi_0,\ \Phi_2(1) = \Phi_s, \tag{8}$$

$$\begin{gathered} \frac{d\Phi_1(y)}{dy}|_{y=D} - \varepsilon \frac{d\Phi_2(y)}{dy}|_{y=D} = -Q, \\ \Phi_2(D) - \Phi_1(D) = \Delta\Phi, \end{gathered} \tag{9}$$

The general solutions of Eq. (7) along with the boundary conditions (8) and interface fluid-fluid conditions (9) take the form

$$\Phi_i(y) = C_{i1}\cosh(k_i y) + C_{i2}\sinh(k_i y),\ \ i = 1,2, \tag{10}$$

where

$$C_{11} = \Phi_0$$

$$C_{12} = \frac{-\varepsilon\Phi_s k_2 + \varepsilon k_2(\Delta\Phi + \Phi_0\cosh(Dk_1))\cosh(k_2(1-D)) + (Q + \Phi_0 k_1\sinh(Dk_1))\sinh(k_2(1-D))}{-\varepsilon k_2\cosh(k_2(1+D))\sinh(k_1 D) + k_1\cosh(k_1 D)\sinh(k_2(1-D))}$$

$$C_{21} = \frac{-\varepsilon\Phi_s k_2\cosh(k_2 D)\sinh(k_1 D) - k_1(\Phi_0 + \Delta\Phi\cosh(k_1 D))\sinh(k_2) + Q\sinh(k_1 D)\sinh(k_2) + \Phi_s k_1\cosh(k_1 D)\sinh(k_2 D)}{-\varepsilon k_2\cosh(k_2(1+D))\sinh(k_1 D) + k_1\cosh(k_1 D)\sinh(k_2(1-D))} \tag{11}$$

$$C_{22} = \frac{-\Phi_s k_1\cosh(k_1 D)\cosh(k_2 D) + \cosh(k_2)(\Phi_0 k_1 + \Delta\Phi k_1\cosh(k_1 D) - Q\sinh(k_1 D)) + \varepsilon\Phi_s k_2\sinh(k_1 D)\sinh(k_2 D)}{-\varepsilon k_2\cosh(k_2(1+D))\sinh(k_1 D) + k_1\cosh(k_1 D)\sinh(k_2(1-D))}$$

## 3. Velocity distributions

The fluids are assumed to be immiscible and incompressible and the flow is unsteady, fully developed and one dimensional. The electroosmotic flows of the fluids are generated by the time-dependent pressure gradient in the flow direction and the applied DC electric current of magnitude $E$. The continuity equation is identically satisfied by velocities $v_i'(y',t'), i=1,2$ of both layers. The governing equations of motion along with initial, boundary and the interface fluid-fluid conditions are

the system of linear momentum equations

$$\rho_i \frac{\partial v_i'}{\partial t'} = \frac{\partial \tau_i'}{\partial y'} - \frac{\partial p'}{\partial x'} + \rho_{e_i}'(y')E, \ \ i=1,2, \tag{12}$$

the system of constitutive equations

$$\tau_i' = \mu_i \frac{\partial v_i'}{\partial y'}, \ \ i=1,2, \tag{13}$$

the initial conditions

$$v_i'(y',0)=0, \ \tau_i'(y',0)=0, \ i=1,2, \tag{14}$$

the Robin boundary conditions

$$v_1'(0,t') - l_1 \frac{\partial v_1'(y',t')}{\partial y'}|_{y'=0} = V_0 \overline{f}_1(t'), \tag{15}$$

$$v_2'(d,t') + l_2 \frac{\partial v_2'(y',t')}{\partial y'}|_{y'=d} = V_0 \overline{f}_2(t'),$$

the interfacial fluid-fluid conditions

$$\begin{gathered} v_1'(d_1,t') = v_2'(d_1,t'), \\ \left(\varepsilon_1 E \frac{\partial \Phi_1'(y')}{\partial y'} - \mu_1 \frac{\partial v_{1'}(y',t')}{\partial y'}\right)_{y'=d_1} = \left(\varepsilon_2 E \frac{\partial \Phi_2'(y')}{\partial y'} - \mu_2 \frac{\partial v_{2'}(y',t')}{\partial y'}\right)_{y'=d_1} \end{gathered} \tag{16}$$

With the help of Eqs. (1), (3) and (13), Eq. (12) takes the form

$$\rho_i \frac{\partial v_i'}{\partial t'} = \mu_i \frac{\partial^2 v_i'}{\partial y'^2} - \frac{\partial p'}{\partial x'} - EK_i^2 \varepsilon_i \Phi_i'(y'), \ \ i=1,2. \tag{17}$$

In this paper we consider the pressure gradient $-\frac{\partial p'}{\partial x'} = P_0 p'(t')$. Using Eq. (6) and the following dimensionless parameters,

$$x=\frac{x'}{d}, v=\frac{v'}{V_0}, t=\frac{V_0 t'}{d}, a_i=\frac{P_0 d}{V_0^2\rho_i}, b_i=\frac{\nu_i}{dV_0}$$
$$c_i=\frac{2n_0 Eedz_\nu}{\rho_i V_0^2}, \gamma_1=\frac{l_1}{d}, \gamma_2=\frac{l_2}{d}, f_1(t)=f_1'(\frac{dt}{V_0}), f_2(t)=f_2'(\frac{dt}{V_0}) \quad (18)$$
$$\alpha_1=\frac{\varepsilon_1 EK_B T_0}{\mu_1 V_0 z_\nu e}, \alpha_2=\frac{\varepsilon_2 EK_B T_0}{\mu_1 V_0 z_\nu e}, \mu=\frac{\mu_2}{\mu_1}, p=\frac{p'}{dP_0}, \ i=1,2.$$

Eqs. (17), (14), (15) and (16) in dimensionless form reduce to

$$\frac{\partial v_1}{\partial t}=b_1\frac{\partial^2 v_1}{\partial y^2}+a_1P(t)-c_1\Phi_1(y), \quad (19)$$

$$\frac{\partial v_2}{\partial t}=b_2\frac{\partial^2 v_2}{\partial y^2}+a_2P(t)-c_2\Phi_2(y), \quad (20)$$

the initial conditions

$$v_i(y,0)=0, \ i=1,2 \quad (21)$$

the Robin boundary conditions

$$v_1(0,t)-\gamma_1\frac{\partial v_1(y,t)}{\partial y}|_{y=0}=f_1(t), \quad (22)$$

$$v_1(1,t)+\gamma_2\frac{\partial v_2(y,t)}{\partial y}|_{y=1}=f_2(t),$$

the interfacial fluid-fluid conditions

$$v_1(D,t)=v_2(D,t),$$
$$\left(\alpha_1\frac{\partial\Phi_1(y)}{\partial y}-\frac{\partial v_1(y,t)}{\partial y}\right)_{y=D}=\left(\alpha_2\frac{\partial\Phi_2(y)}{\partial y}-\mu\frac{\partial v_2(y,t)}{\partial y}\right)_{y=D}, \quad (23)$$

where $-\frac{\partial p}{\partial x}=P(t)$. Applying the Laplace transform to Eqs. (19), (20), (22) and (23) along with the initial conditions (21), we can write

$$b_1\frac{\partial^2\overline{v}_1}{\partial y^2}-q\overline{v}_1=\frac{c_1}{q}\Phi_1(y)-a_1\overline{P}(q), \quad (24)$$

$$b_2\frac{\partial^2\overline{v}_2}{\partial y^2}-q\overline{v}_2=\frac{c_2}{q}\Phi_2(y)-a_2\overline{P}(q), \quad (25)$$

$$\overline{v}_1(0,q)-\gamma_1\frac{\partial\overline{v}_1(y,q)}{\partial y}|_{y=0}=\overline{f}_1(q), \quad (26)$$

$$\overline{v}_1(1,q)+\gamma_2\frac{\partial\overline{v}_2(y,q)}{\partial y}|_{y=1}=\overline{f}_2(q),$$

$$\overline{v}_1(D,q)=\overline{v}_2(D,q),$$

$$\left(\frac{\alpha_1}{q}\frac{\partial\Phi_1(y)}{\partial y}-\frac{\partial\overline{v}_1(y,q)}{\partial y}\right)_{y=D}=\left(\frac{\alpha_2}{q}\frac{\partial\Phi_2(y)}{\partial y}-\mu\frac{\partial\overline{v}_2(y,q)}{\partial y}\right)_{y=D}, \tag{27}$$

where $\overline{v}_i(y,q)=\int_0^\infty e^{-qt}v_i(y,t)dt,$ i=1,2. The general solutions of Eqs. (24) and (25}) are

$$\overline{v}_1(y,q)=A_1e^{-y\sqrt{\frac{q}{b_1}}}+A_2e^{y\sqrt{\frac{q}{b_1}}}+\frac{c_1}{q(b_1k_1^2-q)}\Phi_1(y)+\frac{a_1}{q}\overline{P}(q) \tag{28}$$

$$\overline{v}_2(y,q)=B_1e^{-y\sqrt{\frac{q}{b_2}}}+B_2e^{y\sqrt{\frac{q}{b_2}}}+\frac{c_2}{q(b_2k_2^2-q)}\Phi_2(y)+\frac{a_2}{q}\overline{P}(q) \tag{29}$$

The constants $A_1,A_2,B_1,B_2$ are determined by applying the transformed robin boundary condition (26) and the transformed fluid-fluid interface conditions (27) and are given by the following linear system,

$$B=M^{-1}F, \tag{30}$$

where

$$M=\begin{pmatrix}
1+\gamma_1\sqrt{\frac{q}{b_1}} & 1-\gamma_1\sqrt{\frac{q}{b_1}} & 0 & 0\\
0 & 0 & (1-\gamma_2\sqrt{\frac{q}{b_2}})e^{-\sqrt{\frac{q}{b_2}}} & (1+\gamma_2\sqrt{\frac{q}{b_2}})e^{\sqrt{\frac{q}{b_2}}}\\
e^{-D\sqrt{\frac{q}{b_1}}} & e^{D\sqrt{\frac{q}{b_1}}} & -e^{-D\sqrt{\frac{q}{b_2}}} & -e^{D\sqrt{\frac{q}{b_2}}}\\
\sqrt{\frac{q}{b_1}}e^{-D\sqrt{\frac{q}{b_1}}} & -\sqrt{\frac{q}{b_1}}e^{D\sqrt{\frac{q}{b_1}}} & -\mu\sqrt{\frac{q}{b_2}}e^{-D\sqrt{\frac{q}{b_2}}} & \mu\sqrt{\frac{q}{b_2}}e^{D\sqrt{\frac{q}{b_2}}}
\end{pmatrix},$$

$$B=\begin{pmatrix}A_1\\A_2\\B_1\\B_2\end{pmatrix},\quad F=\begin{pmatrix}F_1(q)\\F_2(q)\\F_3(q)\\F_4(q)\end{pmatrix}, \tag{31}$$

$$F_1(q)=\bar{f}_1(q)-\frac{c_1\Phi_1(0)}{q(b_1k_1^2-q)}+\gamma_1\frac{c_1}{q(b_1k_1^2-q)}\frac{d\Phi_1(y)}{dy}|_{y=0}-\frac{a_1}{q}\bar{P}(q),$$

$$F_2(q)=\bar{f}_2(q)-\frac{c_2\Phi_2(1)}{q(b_2k_2^2-q)}-\gamma_2\frac{c_2}{q(b_2k_2^2-q)}\frac{d\Phi_2(y)}{dy}|_{y=1}-\frac{a_2}{q}\bar{P}(q),$$

$$F_3(q)=\frac{(a_2-a_1)\bar{P}(q)}{q}+\frac{c_2\Phi_2(D)}{q(b_2k_2^2-q)}-\frac{c_1\Phi_1(D)}{q(b_1k_1^2-q)},$$

$$F_4(q)=\frac{\alpha_2}{q}\frac{d\Phi_2(y)}{dy}|_{y=D}-\frac{\mu c_2}{q(b_2k_2^2-q)}\frac{d\Phi_2(y)}{dy}|_{y=D}-\frac{\alpha_1}{q}\frac{d\Phi_1(y)}{dy}|_{y=D}+\frac{c_1}{q(b_1k_1^2-q)}\frac{d\Phi_1(y)}{dy}|_{y=D}$$

After having determined the parameters $A_i, B_i, i=1,2$, from the system (30) and (31) the analytic solution for the velocity distributions $v_i(y,t)$, $i=1,2,$ can be determined by applying the inverse Laplce transform to Eq. (28) and (29)

$$v_i(y,t)=\frac{1}{2\pi\imath}\int_{\sigma-\imath\infty}^{\sigma+\imath\infty}e^{st}\bar{v}_i(y,q)dq,\ i=1,2, \tag{32}$$

where $\imath=\sqrt{-1}$. In this paper, the inverse Laplace transforms are obtained by using numerical algorithm such as Talbot's algorithms [23,24].

Let $\bar{G}(y,s)$ be the Laplace transform of the function $g(y,t)$. The function $g(y,t)$ can be approximated with the help of Talbot algorithm [23] for the Laplace transform inversion,

$$g(y,t)\cong\frac{r}{M}\left\{\frac{\exp(rt)}{2}\bar{G}(y,r)+\sum_{k=1}^{M-1}\mathrm{Re}\left[\exp(tz(\theta_k))\bar{G}(y,z(\theta_k))\left(1+i\zeta(\theta_k)\right)\right]\right\}, \tag{33}$$

where

$$r=\frac{2M}{5t},\ z(\theta)=r\theta(\cot\theta+i),\ \theta\in(-\pi,\pi), \tag{34}$$

$$\zeta(\theta)=\theta+(\theta cot\theta-1)cot\theta,\theta_k=\frac{k\pi}{M}.$$

Another method to approximate the function $g(y,t)$ is the improved Talbot algorithm for the inverse Laplace transform and is given by [24]

$$g(y,t)\cong\frac{1}{t}\sum_{k=1}^{M}\exp(tz_1(\sigma_k))\bar{G}(y,z_1(\sigma_k))\left(\nu+i\zeta_1(\sigma_k)\right), \tag{35}$$

where,

$$z_1(\theta) = \frac{M}{t}\left[\nu i\theta + \mu\theta\cot(\alpha\theta) - \xi\right],\ \theta \in [-\pi, \pi],$$

$$\zeta_1(\theta) = \alpha\mu\theta + \mu(\alpha\theta cot(\alpha\theta) - 1)cot(\alpha\theta), \sigma_k = \frac{(2k-1)\pi}{M} - \pi. \tag{36}$$

Here $\alpha$, $M$, $\nu$, $\mu$, $\xi$ are parameters to be specified by the user.

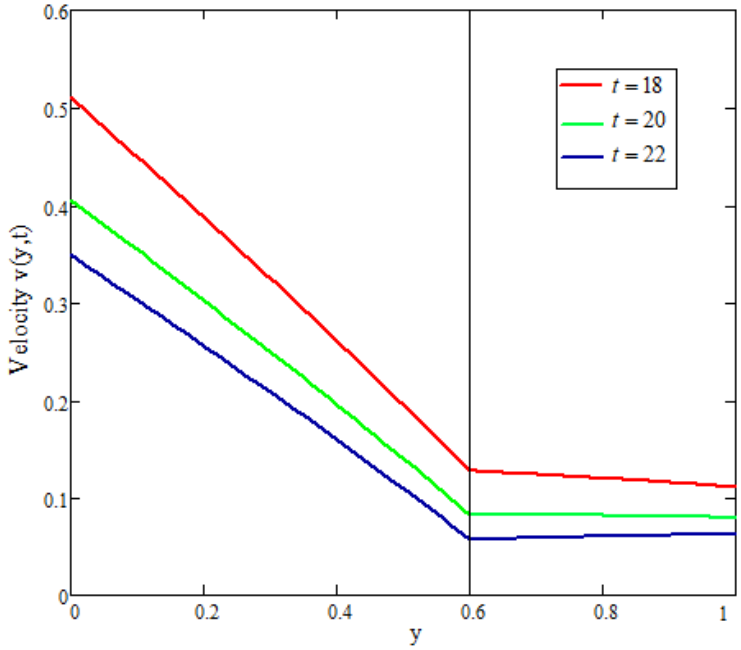


Figure 2: Velicity profile $v_i(y,t)$, $i = 1,2$ versus $y$ for 2-layers electo osmotic fluid at $\varepsilon = 1$, $\Delta\Phi = 1.5$, $\gamma_1 = 0.05$, $\gamma_2 = 0.05$, $\alpha_1 = 0.5$, $\alpha_2 = 0.75$, $\omega = \frac{\pi}{6}$ and $Q = 2$ for different values of $t$.

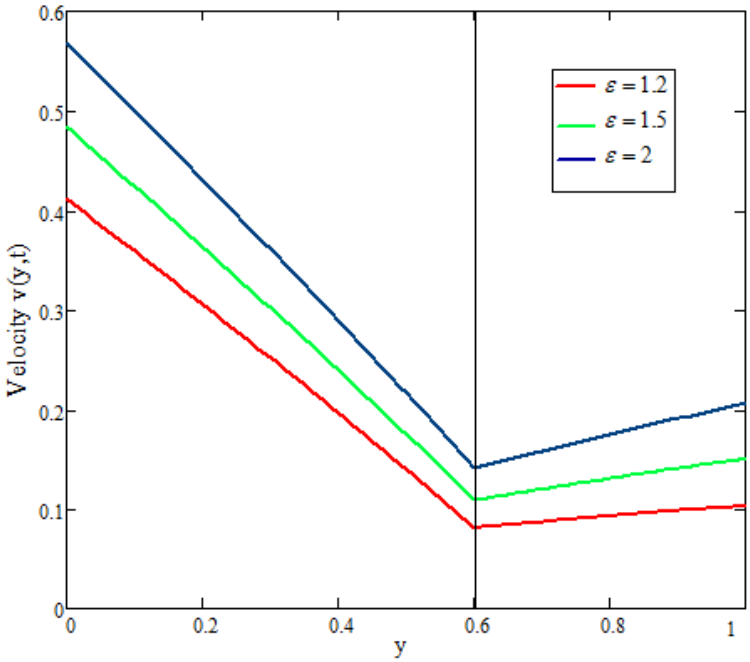


Figure 3: Velicity profile $v_i(y,t)$ $i = 1,2$ versus $y$ for 2-layers electo osmotic fluid at $t = 22$, $\Delta\Phi = 1.5$, $\gamma_1 = 0.05$, $\gamma_2 = 0.05$, $\alpha_1 = 0.5$, $\alpha_2 = 0.75$, $\omega = \frac{\pi}{6}$ and $Q = 2$ for different values of $\varepsilon$.

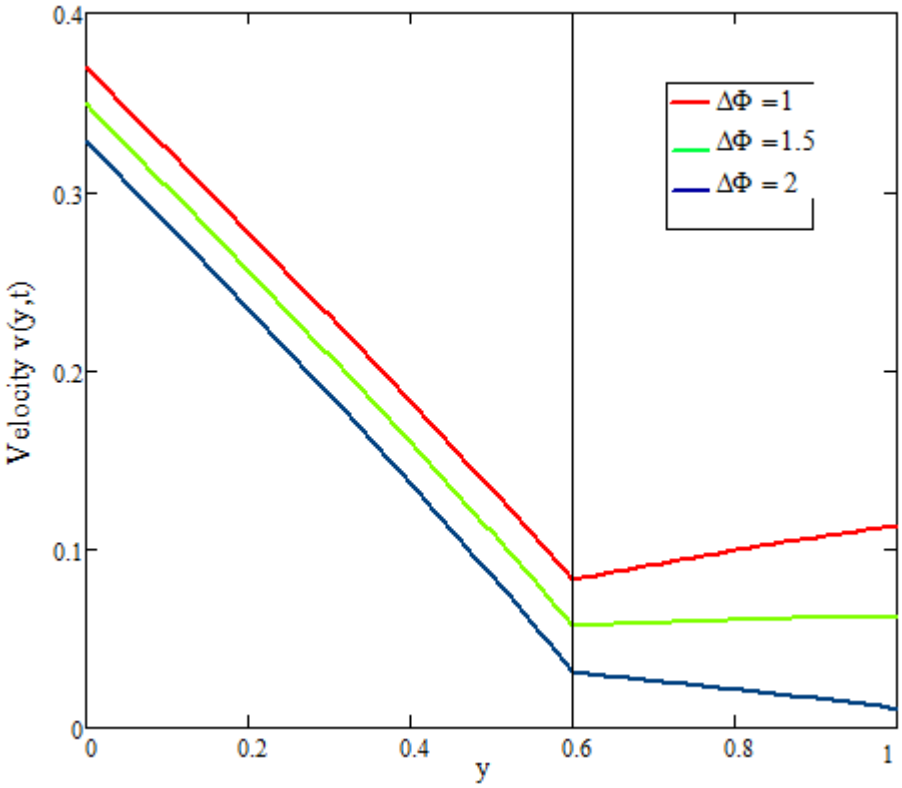


Figure 4: Velicity profile $v_i(y,t)$ $i = 1,2$ versus $y$ for 2-layers electo osmotic fluid at $t = 22$, $\varepsilon = 1$, $\gamma_1 = 0.05$, $\gamma_2 = 0.05$, $\alpha_1 = 0.5$, $\alpha_2 = 0.75$, $\omega = \frac{\pi}{6}$ and $Q = 2$ for different values of

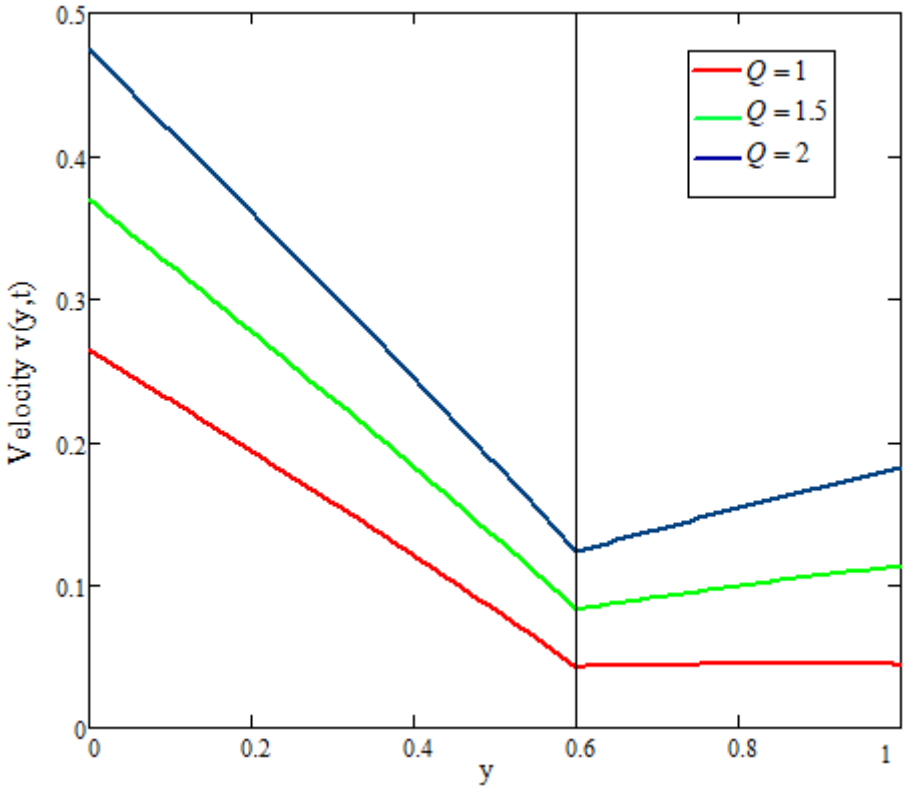


$\Delta\Phi$.

Figure 5: Velicity profile $v_i(y,t)$ $i = 1,2$ versus $y$ for 2-layers electo osmotic fluid at $t = 22$, $\varepsilon = 1$, $\gamma_1 = 0.05$, $\gamma_2 = 0.05$, $\alpha_1 = 0.5$, $\alpha_2 = 0.75$, $\omega = \frac{\pi}{6}$ and $\Delta\Phi = 1$ for different values of $Q$.

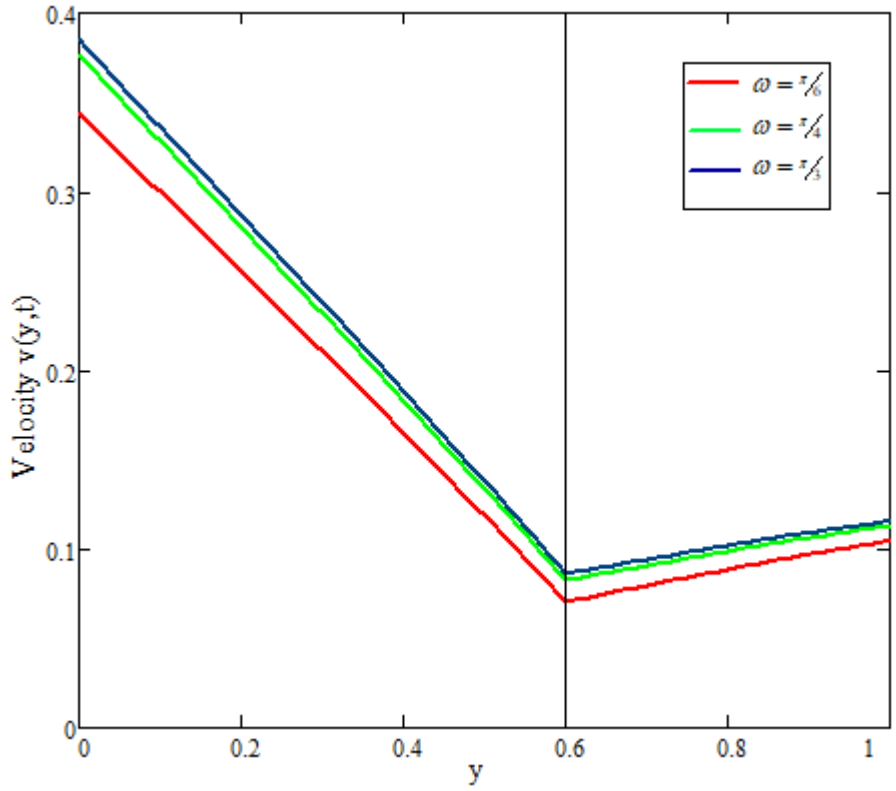


Figure 6: Velicity profile $v_i(y,t)$ $i = 1,2$ versus $y$ for 2-layers electo osmotic fluid at $t = 25$, $\varepsilon = 1$, $\gamma_1 = 0.05$, $\gamma_2 = 0.05$, $\alpha_1 = 0.5$, $\alpha_2 = 0.75$, $Q = 2$ and $\Delta\Phi = 1$ for different values of $\omega$.

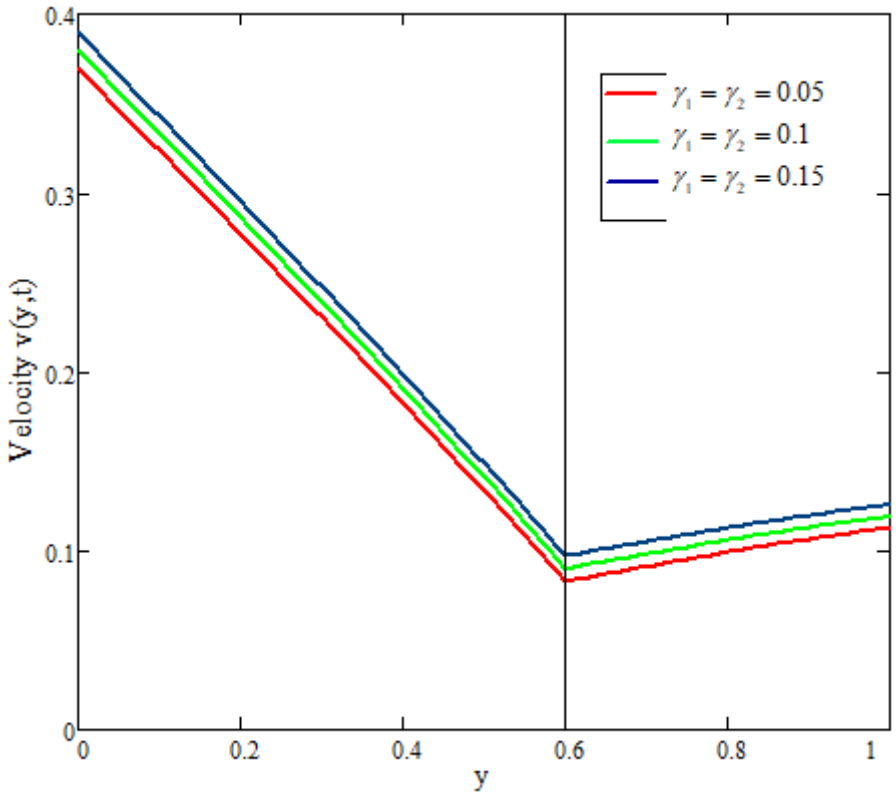


Figure 7: Velicity profile $v_i(y,t)$ $i = 1,2$ versus $y$ for 2-layers electo osmotic fluid at $t = 22$, $\varepsilon = 1$, $\omega = \frac{\pi}{6}$, $\alpha_1 = 0.5$, $\alpha_2 = 0.75$, $Q = 2$ and $\Delta\Phi = 1$ for different values of $\gamma_1 = \gamma_2$.

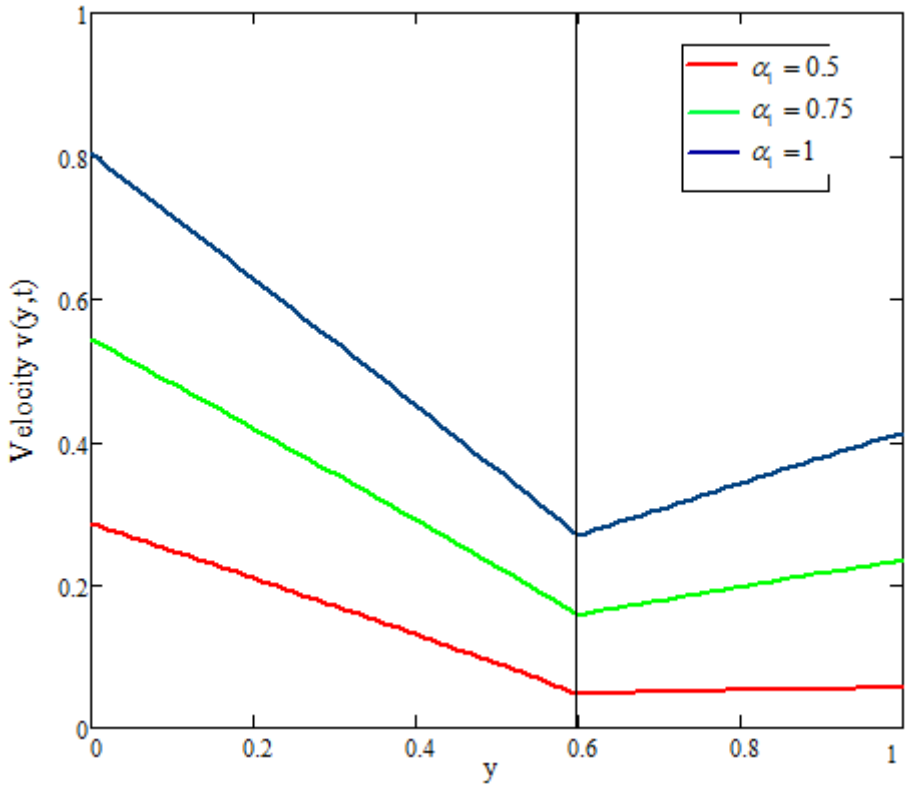


Figure 8: Velicity profile $v_i(y,t)$ $i = 1,2$ versus $y$ for 2-layers electo osmotic fluid at $t = 22$, $\varepsilon = 1$, $\gamma_1 = 0.05$, $\gamma_2 = 0.05$, $\omega = \frac{\pi}{6}$, $\alpha_2 = 1$, $Q = 2$ and $\Delta\Phi = 1$ for different values of $\alpha_1$.

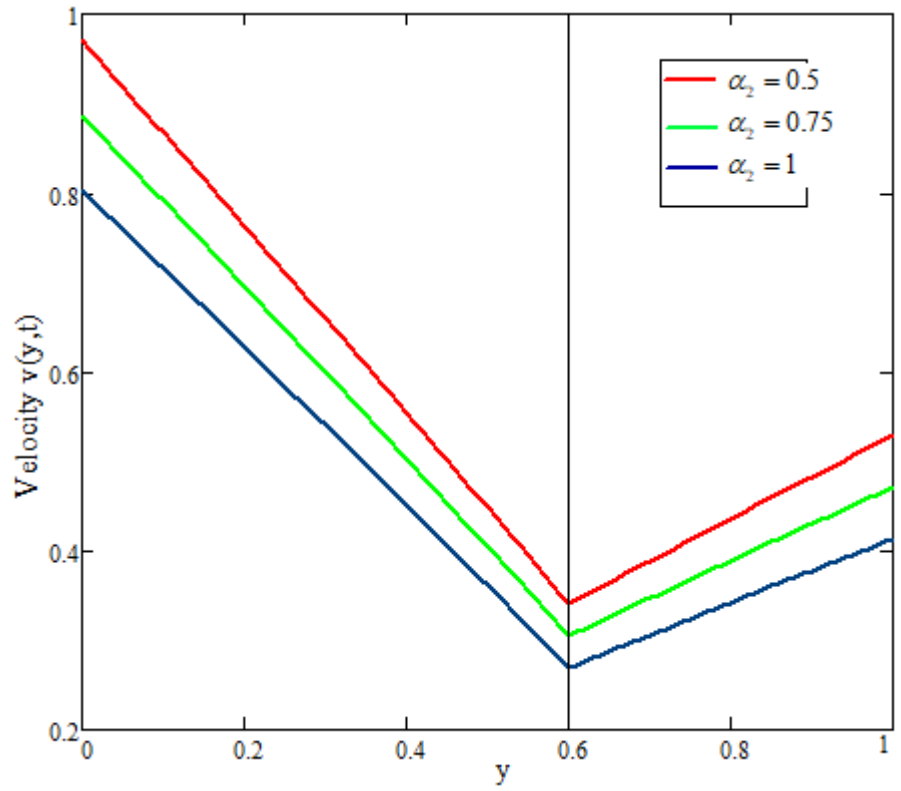


Figure 9: Velicity profile $v_i(y,t)$ $i = 1,2$ versus $y$ for 2-layers electo osmotic fluid at $t = 22$, $\varepsilon = 1$, $\gamma_1 = 0.05$, $\gamma_2 = 0.05$, $\omega = \frac{\pi}{6}$, $\alpha_1 = 1$, $Q = 2$ and $\Delta\Phi = 1$ for different values of $\alpha_2$.

## 4. Numerical results and discussion

In this paper we have acquired the semi-analytical solution for the velocity profile corresponding to electroosmosis and pressure driven flow of two layer Newtonian fluid under the influence of zeta potential difference and Maxwell interfacial stress. For numerical illustration, we used the function $p(t) = e^{-2t}$, $f_1(t) = \sin\omega t$ and $f_1(t) = \frac{1}{4}\sin 2\omega t$, where $\omega$ represent the angular frequency of oscillation. We have analyzed graphical the effects of time variation $t$, dielectric constant ratio $\varepsilon$, interface zeta potential difference $\Delta\Phi$, interface charge density $Q$, slip parameters $\gamma_1, \gamma_2$, angular frequency $\omega$, and other physical parameters $\alpha_1, \alpha_2$. For graphical interpretation of the obtained results we used the values $D = 0.6$, $a_1 = 0.005333$, $a_2 = 0.003692$, $b_1 = 1$, $b_2 = 2$,, $c_1 = 0.2$, $c_2 = 0.5$, $k_1 = 2$, $k_2 = 3$, $\Phi_0 = 0.4$, $\Phi_s = -0.5$ and $\mu = 2.889$ for the non-dimensional parameters.

Fig. 2 demonstrates the time effect on the electro-osmotic velocity profile. From Fig. 2 it can be observed the velocity decreases with the increase in time $t$ and with the passage of time velocity becomes steady. Fig. 3 represents the effect of the dielectric constant ratio of the second layer for the first layer on the fluid velocity. It is observed that fluid velocity in both layers increases with the increase in a dielectric constant ratio of $\varepsilon$. Fig. 4 exhibits the influence of interface zeta potential difference $\Delta\Phi$ to the double layer electroosmotic velocity. It can be seen from the graph that the fluid velocity decreases with the increase in the interface zeta potential difference. The effect of non-dimensional interface charge density jump $Q$ on the 2-layer fluid flow is examined in Fig. 5. It has been observed that with the enhancement in the interface charge density $Q$, the fluid velocity enhanced. Fig. 6 represents the angular frequency $\omega$ effect on the velocity profile. It can be seen from the graph that the velocity profile increases with the increase in $\omega$. Fig. 7 reveals the fluid-liquid slip velocity parameters $\gamma_1$, $\gamma_2$ effect on the electroosmotic velocity profile. It is observed that the velocity profile increases slowly with the increase in fluid-liquid slip velocity parameters. Figs. 8 and 9 demonstrate the effects of the physical parameters $\alpha_1$ and $\alpha_2$ on the electroosmotic velocity. It has been noted from that graphs that electroosmotic mobility enhances with the increase in $\alpha_1$ and descends with the increase in $\alpha_2$.

## References

[1] Stone, H.A., Stroock, A.D. and Ajdari, A., 2004. Engineering flows in small devices: microfluidics toward a lab-on-a-chip. Annu. Rev. Fluid Mech., 36, pp.381-411.

[2] Hunter, R. J. (1981). Zeta potential in colloid science. Academic, San Diego.

[3] Karniadakis, G., Beskok, A. and Aluru, N., 2006. Microflows and nanoflows: fundamentals and simulation (Vol. 29). Springer Science & Business Media.

[4] Chang, H.T., Chen, H.S., Hsieh, M.M. and Tseng, W.L., 2000. Electrophoretic separation of DNA in the presence of electroosmotic flow. Reviews in Analytical Chemistry, 19(1), pp.45-74.

[5] Anderson, G.P., King, K.D., Cuttino, D.S., Whelan, J.P., Ligler, F.S., MacKrell, J.F., Bovais, C.S., Indyke, D.K. and Foch, R.J., 1999. Biological agent detection with the use of an airborne biosensor. Field Analytical Chemistry & Technology, 3(4-5), pp.307-314.

[6] Chen, C.H., Zeng, S., Mikkelsen, J.C. and Santiago, J.G., 2000, November. Development of a planar electrokinetic micropump. In Proc of ASME Int Mech Eng Congress and Exposition (pp. 523-528).

[7] Dutta, P. and Beskok, A., 2001. Analytical solution of time periodic electroosmotic flows: analogies to Stokes' second problem. Analytical Chemistry, 73(21), pp.5097-5102.

[8] Wang, X., Chen, B. and Wu, J., 2007. A semianalytical solution of periodical electro-osmosis in a rectangular microchannel. Physics of Fluids, 19(12), p.127101.

[9] Jian, Y., Yang, L. and Liu, Q., 2010. Time periodic electro-osmotic flow through a microannulus. Physics of Fluids, 22(4), p.042001.

[10] Liu, Q.S., Jian, Y.J. and Yang, L.G., 2011. Time periodic electroosmotic flow of the generalized Maxwell fluids between two micro-parallel plates. Journal of Non-Newtonian Fluid Mechanics, 166(9-10), pp.478-486.

[11] Jian, Y.J., Liu, Q.S. and Yang, L.G., 2011. AC electroosmotic flow of generalized Maxwell fluids in a rectangular microchannel. Journal of Non-Newtonian Fluid Mechanics, 166(21-22), pp.1304-1314.

[12] Su, J., Jian, Y. and Chang, L., 2012. Thermally fully developed electroosmotic flow through a rectangular microchannel. International Journal of Heat and Mass Transfer, 55(21-22), pp.6285-6290.

[13] Keh, H.J. and Tseng, H.C., 2001. Transient electrokinetic flow in fine capillaries. Journal of colloid and Interface Science, 242(2), pp.450-459.

[14] Deng, S.Y., Jian, Y.J., Bi, Y.H., Chang, L., Wang, H.J. and Liu, Q.S., 2012. Unsteady electroosmotic flow of power-law fluid in a rectangular microchannel. Mechanics Research Communications, 39(1), pp.9-14.

[15] Brask, A., Goranovic, G. and Bruus, H., 2003. Electroosmotic pumping of nonconducting liquids by viscous drag from a secondary conducting liquid. Tech Proc Nanotech, 1, pp.190-193.

[16] Shankar, V. and Sharma, A., 2004. Instability of the interface between thin fluid films subjected to electric fields. Journal of colloid and interface science, 274(1), pp.294-308.

[17] Verma, R., Sharma, A., Kargupta, K. and Bhaumik, J., 2005. Electric field induced instability and pattern formation in thin liquid films. Langmuir, 21(8), pp.3710-3721.

[18] Liu, M., Liu, Y., Guo, Q. and Yang, J., 2009. Modeling of electroosmotic pumping of nonconducting liquids and biofluids by a two-phase flow method. Journal of electroanalytical chemistry, 636(1-2), pp.86-92.

[19] Gao, Y., Wong, T.N., Yang, C. and Ooi, K.T., 2005. Transient two-liquid electroosmotic flow with electric charges at the interface. Colloids and Surfaces A: Physicochemical and Engineering Aspects, 266(1-3), pp.117-128.

[20] Su, J., Jian, Y.J., Chang, L. and Li, Q.S., 2013. Transient electro-osmotic and pressure driven flows of two-layer fluids through a slit microchannel. Acta Mechanica Sinica, 29(4), pp.534-542.

[21] Goswami, P. and Chakraborty, S., 2011. Semi-analytical solutions for electroosmotic flows with interfacial slip in microchannels of complex cross-sectional shapes. Microfluidics and nanofluidics, 11(3), pp.255-267.

[22] Shit, G.C., Mondal, A., Sinha, A. and Kundu, P.K., 2016. Effects of slip velocity on rotating electro-osmotic flow in a slowly varying micro-channel. Colloids and Surfaces A: Physicochemical and Engineering Aspects, 489, pp.249-255.

[23] J. Abate, P. P. Valko, Multi-precision Laplace transform inversion, Int. J. Numer. Meth. Engng., 60 (2004) 979-993, doi:10.1002/nme.995.

[24] B. Dingfelder, J. A. C. Weideman, An improved Talbot method for numerical Laplace transform inversion, Numer. Algor., 68 (2015) 167-183, doi: 10.1007/s11075-014-9895-z.